LIDAR INVESTIGATIONS OF PARTICLES ORIENTATION IN CRYSTAL CLOUDS

B.V. Kaul', O.A. Krasnov, A.L. Kuznetsov, E.R. Polovtseva, I.V. Samokhvalov, and A.P. Stykon

Institute of Atmospheric Optics, Siberian Branch of the Russian Academy of Sciences, Tomsk

Received September 27, 1996

We present here some measurement results on the backscattering phase matrices (BSPM) of crystal clouds. The measurements were carried out with a lidar the Stokes parameters of the sounding beam in which can be varied and all Stokes parameters of lidar returns are measured. The BSPMs often have the nondiagonal form, what is caused by the presence of preferred orientation of scattering particles. The direction and degree of the particle orientation are estimated from the measurement results. The consequence of the orientation of crystal cloud particles is the essential anisotropy of the backscattering coefficient related to the polarization state of the sounding beam and the direction of its incidence on the cloud layer, that is illustrated by some examples.

Particles of crystal clouds have a well pronounced anisotropy of their size. In contrast to droplet clouds, optical properties of which, at the known refractive index, are determined only by the particle size-distribution, the additional parameters related to the size and orientation of particles appear in the crystal clouds. As the first approximation, particles may be approximated by the bodies of simple geometric shape, for example, by axially-symmetrical columns and plates. Then the shape parameters are the maximum and minimum size of the particles. The ensemble of particles is described by a two-dimensional particle size-distribution. The orientation state of particles in the ensemble is also characterized by a two-dimensional distribution over polar and azimuth angles of the particle axis position.

If one neglects the aforementioned peculiarities in crystal clouds the correct description of the processes of the electromagnetic radiation scattering seems to be impossible. But, if the shape and size-distribution of particles are investigated by direct methods quite thoroughly, the orientation state of particles in a real cloud remains to be poorly investigated for quite obvious reasons.[1]

The appropriate remote method for obtaining the data on orientation state of particles is the method of lidar measurements of the backscattering phase matrices (BSPM), developed by the authors.[2–4] The lidar providing the application of this method is equipped with a polarization block enabling us to change the sounding beam polarization what makes, together with the polarization analyzer in the lidar receiver, to measure all the Stokes parameters of lidar returns and thus of BSPM.

Two quarter-wave plates are installed on the optical axis of the laser beam *1* (see Fig. 1). They can be turned by a certain set angle around the optical axis. The radiation goes to the atmosphere after passing through the plates and the collimator *2*.

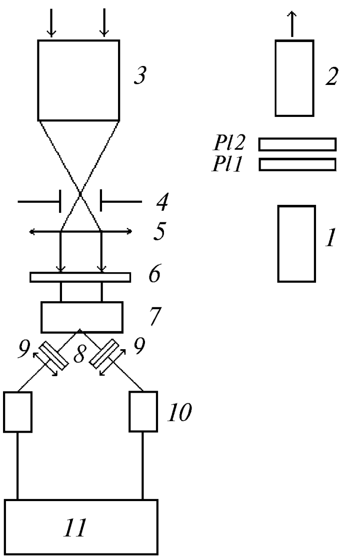

FIG. 1. Block-diagram of the "Stratosfera-1M" polarization lidar: 1) LTI-405 laser; 2) collimator; 3) receiving telescopic antenna; 4) field of view diaphragm; 5) lens; 6) quater-wave plate; 7) Wallastone prism; 8) interference filters; 9) lenses; 10) photomultipliers; 11) lidar recording system; Pl1 and Pl2 are the quater-wave plates.

The scattered radiation coming on the objective *3*, successively passes the field of view diaphragm *4* and the collimating lens *5*. Then it comes to the

0235-6880/97/02 119-07 $02.00

polarization analyzer of the scattered radiation. This unit contains the quater-wave ($\lambda/4$) plate *6* and the Wallastone prism *7*. Both these elements can be turned around the optical axis. The Wallastone prism splits the radiation into two beams with orthogonal linear polarizations. Then these beams pass through the interference filters *8* and are collected by the lenses *9* on the cathodes of photomultipliers FEU-130. The photomultipliers are mounted on the same rotatable platform with the Wallastone prism, and turn together with it. The flux of photocounts comes to a photon counting two-channel system, which distributes the pulses over the temporal strobes so that time position of the strobe determines the distance to the scattering volume.[5] The minimum strobe duration is 80 ns, that corresponds to the range resolution of 12 m. The maximum count rate is 50 MHz. The system of recording, displaying and primary processing the data is constructed based on the "Elektronika-60" computer.

The main specification of the "Stratosfera-1M" lidar is presented below.

Transmitter

Type of the laser	LTI-405
Radiation wavelength, nm	532
Pulse energy, mJ	up to 40
Pulse duration, nsec	12
Pulse repetition frequency, Hz	12 to 25
Beam divergence after collimation, min of arc	1.5
Polarization of radiation: initial – linear (1 1 0 0) after polarizer: linear (1 –1 0 0), linear (1 0 1 0), circular (1 0 0 1)	
Transformation unit: two quater-wave plates $\lambda/4$	

Receiver

Type of the antenna	Cassegrainian telescope
Antenna diameter, m	0.5
Focal length, m	5.7
Field of view, min of arc	3
FWHM of the interference filters, nm	1.5
Polarization elements: Wallastone prism, quater-wave plate $\lambda/4$	
Detectors: two photomultipliers FEU-130	
Recording system: photon counter with the maximum counting rate of	50 MHz
"Elektronika-60" computer	

The methodical aspects were considered earlier, for example in Ref. 2. So we do not consider them here, and only pay attention to the measurement results. The model of cloud of axially-symmetric columns and the related theoretical ideas developed in Refs. 6 and 7 are also used in the interpretation.

Investigations of the aerodynamics of the cloud crystals, the overview of which has been presented, for example, in Ref. 1, show that when falling down the columnar crystals, change their orientation so that it is ordered with their main axis tending to be disposed horizontally. The degree of ordering increases as the column size increases, and can be disordered again only for very big ($l > 2$ mm) crystals. The plates fall down so that their main axes tend to be oriented vertically.

If one takes into account only this constant orienting factor, one can expect the following ensemble model at sounding along zenith direction (z-axis): the column axes are oriented in the polar angle θ counted from the sounding direction near the direction $\theta = \pi/2$, and the plate axes are oriented near $\theta = 0$. There is no preferable direction on the azimuth angle φ counted in the plane perpendicular the z-axis, and the particle axes are distributed uniformly in that plane. The form of BSPM of such an ensemble can be predicted based on quite general symmetry relationships for the BSPM elements of one symmetrical particle and symmetry of the ensemble.[8] The matrix should be diagonal, and the relationship should hold for its diagonal elements m_{22} and m_{33}: $|m_{22}| = |m_{33}|$. An example of the experimentally measured matrix under conditions close to these ones can be seen in Fig. 2, where the vertical profiles of nine independent elements of normalized BSPM are shown. Normalizing was done to the element M_{11} so that for the normalized matrix $m_{11} \equiv 1$ and $|m_{ij}| \le 1$. Six off-diagonal elements of the BSPM not presented in Fig. 2 are determined from the conditions

$$m_{ij} = m_{ji}, \text{ if } i \text{ or } j \ne 3,$$

$$m_{ij} = -m_{ji}, \text{ if } i \text{ or } j = 3.$$

In the case of a BSPM analogous to that presented in Fig. 2, the scattered radiation is partially depolarized, and the polarized component keeps the polarization state of the sounding laser beam. It always happens so that circularly polarized incident radiation undergoes stronger depolarization as compared to that at linearly polarized sounding beam.

It is worth noting here that the theory predicts equality of the elements m_{14} and m_{41} to zero for the ensemble of axially symmetrical particles. It is normally fulfilled in experiments with only rare exceptions. So it is advisable to use the circularly polarized laser radiation in lidars, the polarization characteristics of which are not controlled. It allows one to avoid the ambiguity in the backscattering coefficient which, as it will be shown below, can strongly depend on the polarization state of the sounding beam. The matrices close to that presented in Fig. 2, have been recorded in approximately 60% of the observations.

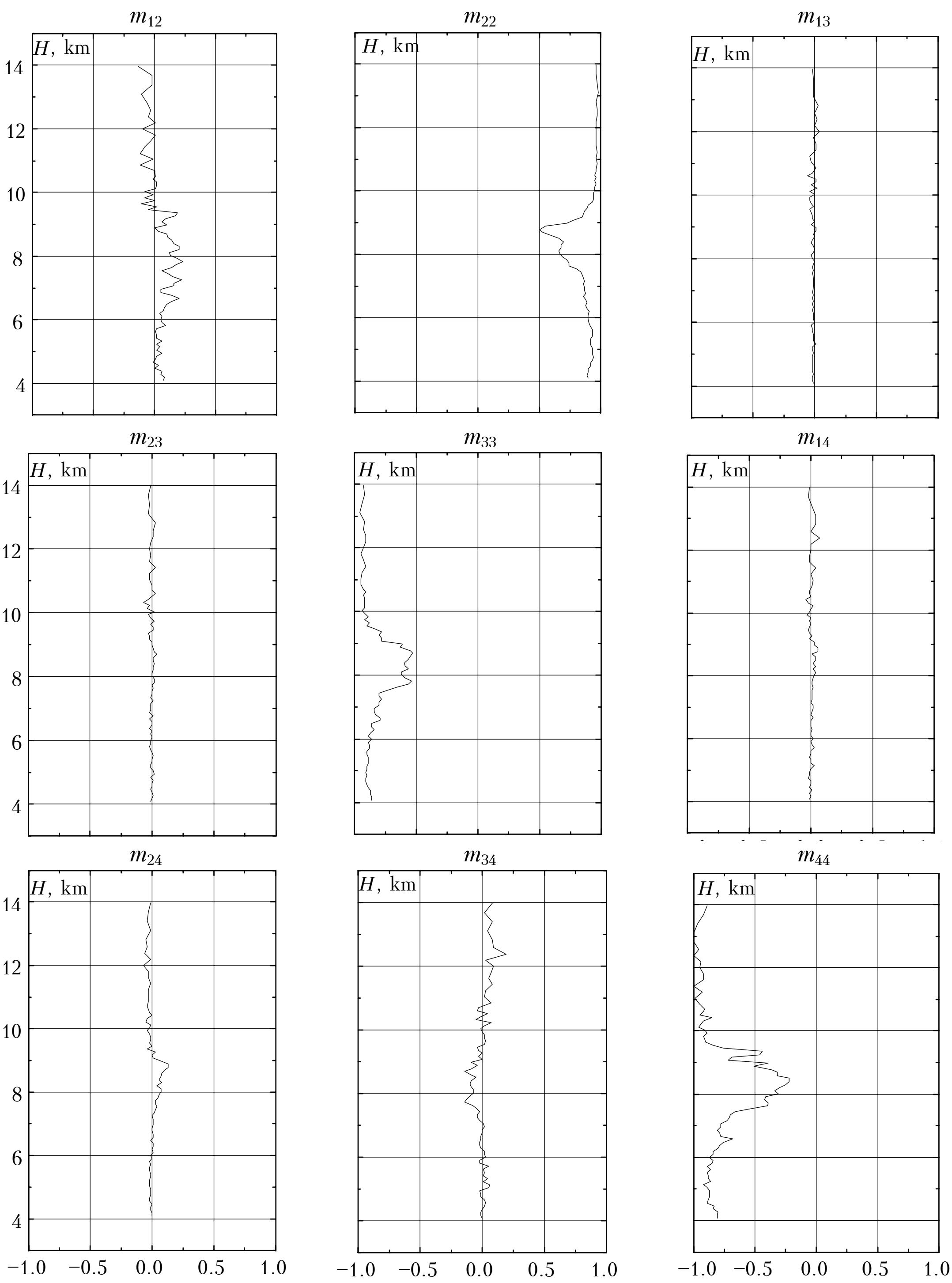

FIG. 2. Example of the elements m_{ij} of the backscattering phase matrix close to the diagonal form.

The next by the frequency of occurrence shape of BSPM, is shown in Fig. 3. Here the elements $m_{12} = m_{21}$ and $m_{34} = -m_{43}$ are significantly different from zero in the layers at the altitudes near 7.5 and 9 km.

One can expect such a shape of BSPM in the frameworks of the accepted model of the ensemble of axially symmetrical particles, if the particle axes tend to group near the reference plane or a plane perpendicular to it, which also contains the direction of sounding. The reference plane, i.e. the plane made of the wave vectors of the incident and scattered waves, is not determined for the backscattering, and any plane including the vectors $\mathbf{k}_0$ and $\mathbf{k}$ can be selected as it, in particular, it can be the *XOZ* plane of the polarization basis of the lidar, as it is accepted in our measurements. This plane is related to the laser transmitter so that its initial linear polarization is described by the normalized Stokes vector $\mathbf{s}_0 = \{1\ 1\ 0\ 0\}^T$. Here T means the transposition.

Let us consider the characteristics of radiation scattered by a layer at the altitude of 7.5 km as an example. The normalized BSPM elements have the following values

$$m_{ij}\,(h = 7.5\ \text{km}) = \begin{pmatrix} 1 & 0.43 & 0 & 0 \\ 0.43 & 0.78 & 0 & 0 \\ 0 & 0 & -0.55 & -0.28 \\ 0 & 0 & 0.28 & -0.35 \end{pmatrix}. \quad (1)$$

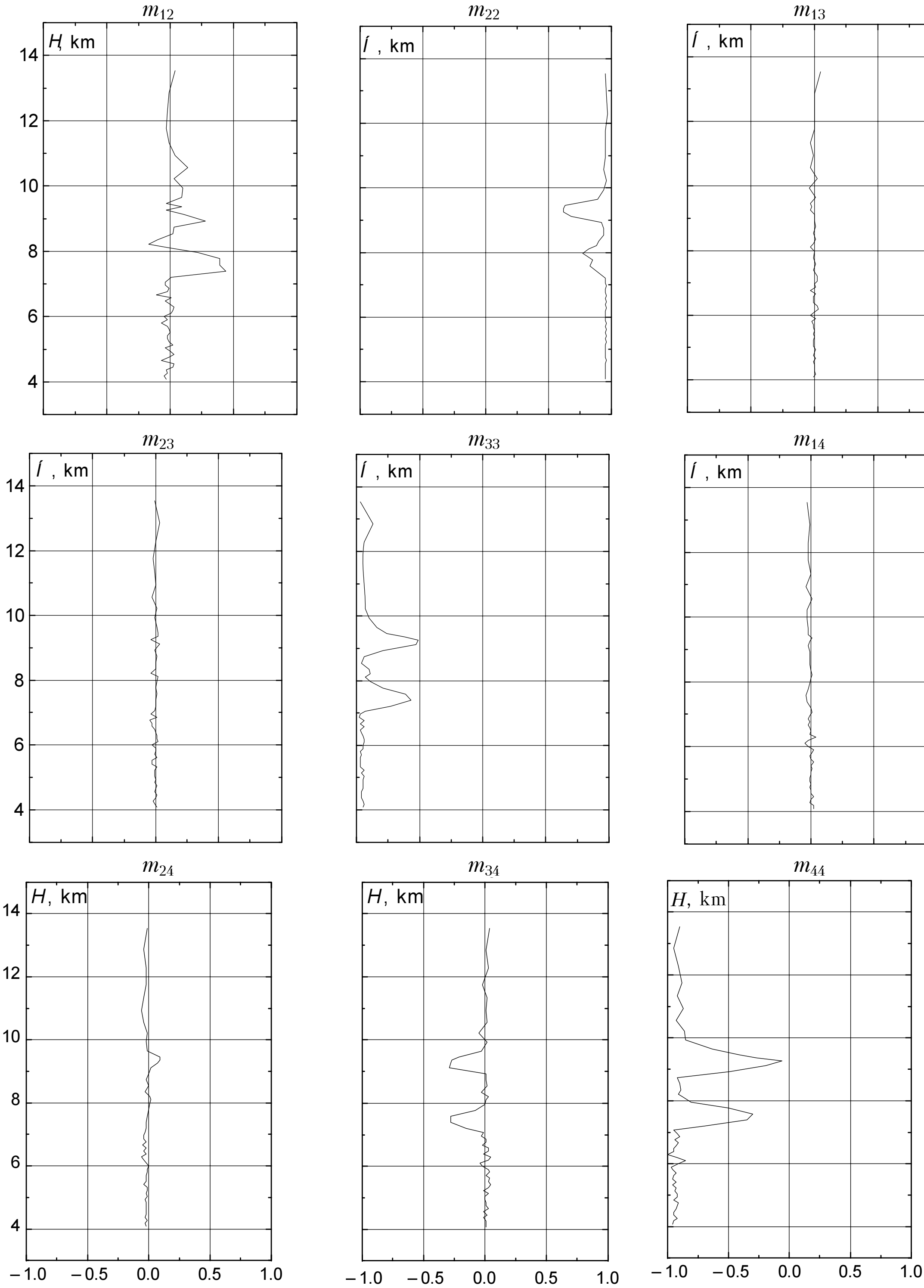

FIG. 3. Example of the off-diagonal BSPM.

Let us now present the normalized Stokes vector as a sum of vectors of completely depolarized and completely polarized radiation

Sounding beam	Scattered beam
$\mathbf{s}_{01} = \{1 \;\; 1\; 0\; 0\}^T$	$\mathbf{s}_1 = 1.43[0.15\{1\;0\;0\;0\}^T + 0.85\{1\;\;1\;0\;0\}^T]$
$\mathbf{s}_{02} = \{1\; -1\; 0\; 0\}^T$	$\mathbf{s}_2 = 0.57[0.39\{1\;0\;0\;0\}^T + 0.61\{1\;-1\;0\;0\}^T]$
$\mathbf{s}_{03} = \{1\; 0\; 1\; 0\}^T$	$\mathbf{s}_3 = [0.39\{1\;0\;0\;0\}^T + 0.61\{1\;0\;-0.90\;\;0.45\}^T]$
$\mathbf{s}_{04} = \{1\;\;0\;0\;-1\}^T$	$\mathbf{s}_4 = [0.65\{1\;0\;0\;0\}^T + 0.35\{1\;0\;0\;-1\}^T]$ (2)

The sum of vectors in square brackets make up unit Stokes vectors and the factors in front of the brackets are the efficiency of the backscattering process for light with the corresponding polarization related to that for natural (unpolarized) light. As is seen, the scattering of radiation with the polarization $\mathbf{s}_{01}$ is 2.5 times more intense relative to the scattering of the orthogonally polarized radiation $\mathbf{s}_{02}$.

The scattering is maximum in the frameworks of the model of axially symmetric particles, when the electric vector of the incident wave is perpendicular to the plane containing the direction of preferred orientation of the main axes of particles. It is observed in the case under consideration. The radiation is depolarized in this case much weaker. The polarization degree is $P = 0.85$, and the polarization state of the polarized component is the same as that of the incident radiation. The latter is also true for $\mathbf{s}_2$ and $\mathbf{s}_4$. In the case of $\mathbf{s}_3$ the elliptization occurs. The depolarization is greater in all three cases than that for $\mathbf{s}_1$, and the circularly polarized radiation is depolarized in the greatest degree, as in the case of random orientation.

The matrix of the form (1) is a particular case of the general BSPM, the direction of preferred orientation of which can be turned on an arbitrary angle relative to the polarization basis of the lidar. The high frequency of occurrence of the BSPM of the form (1) in our measurements can obviously be explained by the fact that the *OX* axis of the polarization basis of the lidar is in the meridian plane, and the most probable direction of preferred orientation is perpendicular to this plane. This fact is possibly connected with the direction of prevailing wind at the altitudes where the crystal clouds are observed.

One can see already from the example (2) that the concept of the lidar depolarization

$$D_l = I_\perp / I_\parallel,$$

i.e. the ratio of the crosspolarized component to the component of the scattered radiation polarized parallel to the linear polarization of sounding radiation, is ambiguous if BSPM is not diagonal. Let us illustrate this by a simple example. If we take the BSPM (1) and apply to it the operation described by the unit vector $\mathbf{s}_{01} = \{1\;1\;0\;1\}^T$, then the normalized Stokes vector of the scattered radiation will have the value

$$\mathbf{s}_1 = \{1,\, q,\, u,\, v\}^t = \{1;\, 0.85;\, 0;\, 0\}^T.$$

As known, the components of the normalized Stokes vector in the representation $\mathbf{I} = \{I_\parallel, I_\perp, u, v\}$ $(I_\parallel + I_\perp = I = 1)$ is expressed in the aforementioned representation as follows:

$$I_\parallel = 1/2\{1 + q\};\; I_\perp = 1/2\{1 - q\}.$$

If we take the value $q = 0.85$, we obtain

$$D_l = I_\perp / I_\parallel = 0.08.$$

Let us assume that the lidar is turned by 90° around the direction of sounding. Then, according to the rules of BSPM transformation (see, for example, Ref. 3), the BSPM (1) is transformed so that it has the same form, but the signs of the elements m_{12}, m_{21} and m_{34}, m_{43} will change. If we make the calculations analogous to the above, then it will occur that $I_\perp/I_\parallel = 0.24$. If the lidar is turned by 45° from the initial position, then $I_\perp/I_\parallel = 0.29$. As follows from this fact, when sounding the crystal clouds, one should be careful formulating conclusions, for example, those concerning the relationship between D_l and the particle size. As it will be shown below, if one forgets that D_l is not the depolarization in its correct understanding, one can come to the physical nonsense when depolarization is greater than 1.

Figure 4 shows the Stokes parameters obtained at sounding crystal clouds. First of all the unusual behavior of the parameter q, which passes to the range of the negative values in the layer at the altitude of 6 km attracts attention. Then the lidar depolarization $D_l = 2.5$, i.e. the readouts in the channel of the crosspolarized radiation is 2.5 times greater than the readouts in the channel measuring the intensity of the component polarized parallel to the linear polarization of the lidar.

Let us consider the characteristics of the scattered radiation and the scattering ensemble based on the estimation of the BSPM obtained in this measurements, which has the form

$$m(h = 7.5\text{ km}) = \begin{pmatrix} 1 & -0.56 & 0.38 & -0.03 \\ -0.56 & 0.37 & -0.21 & 0.20 \\ -0.38 & 0.21 & -0.10 & -0.27 \\ -0.03 & 0.20 & 0.27 & 0.53 \end{pmatrix}. \quad (3)$$

The estimates based on the BSPM model for the axially symmetric particles[7] show that the preferred orientation is turned by the angle $\alpha = 17.5° \pm 0.7°$ relative to the x-axis of the polarization basis of the lidar. The orientation degree is characterized by the Mizes distribution[7] parameter $k = 2.7 \pm 0.3$. It is a high orientation degree, at which the axes of about 90% of particles are oriented within the sector of about the preferred orientation ± 45°.

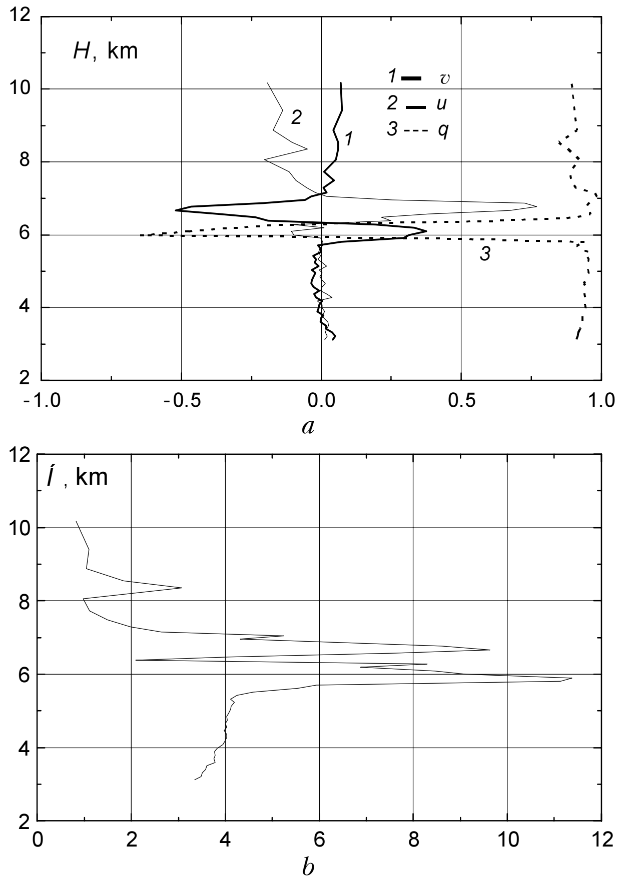

FIG. 4. Profiles of the normalized Stokes parameters q, u, and v obtained from a BSPM measured at illumination of clouds by linearly polarized radiation that has the normalized Stokes vector $\mathbf{s}_{01} = \{1100\}$ *(a) the ratio of the total backscatter to the molecular one, obtained by averaging over three measurements, in which q, u, and v were determined (b).*

Let us consider, how it affects the parameters of scattered radiation. Let us multiply the matrix (3) by the normalized Stokes vector-column $\mathbf{s}_{0i} = \{1\ 1\ 0\ 0\}^{\mathrm{T}}$ and obtain for the backscattered radiation

$\mathbf{s}_1 = 0.44\{1;\ -0.43;\ -0.39;\ 039\}^{\mathrm{T}}$.

The coefficient in front of the normalized Stokes vector means that the intensity of the scattered radiation is 44% of the intensity of scattering of natural light. The scattered light is elliptically polarized. The polarization degree is $P = 0.7$, and, correspondingly, the depolarization is $D = 0.3$. The normalized Stokes vector of the polarized component is equal to

$\mathbf{s}_{1,p} = \{1;\ -0.62;\ -0.56;\ 0.56\}^{\mathrm{T}}$.

The ratio of lengths of the small and big half-axes of the polarization ellipse is $b/a = 0.31$, and the big axis of the ellipse is turned by 21° counterclockwise relative to the positive direction of y axis.

When illuminating the cloud with the radiation having normalized Stokes vector $\mathbf{s}_{02}$, $\mathbf{s}_{03}$, and $\mathbf{s}_{04}$ we obtain the scattered radiation

$\mathbf{s}_2 = 1.53\{1;\ -0.61;\ -0.38;\ -0.15\}$.

The polarization degree is $P = 0.73$. The completely polarized component has the Stokes vector

$\mathbf{s}_{2,p} = \{1;\ -0.84;\ -0.52;\ -0.2\}$.

The polarization ellipse is strongly elongated $b/a = 0.1$ and its big diameter is turned by 16° counterclockwise from the positive direction of the y axis. The scattering is 1.5 times more effective than the scattering of natural light

$\mathbf{s}_3 = 1.38\{1;\ -0.56;\ -0.35;\ 0.17\}$, $P = 0.68$,

$\mathbf{s}_{3,p} = \{1;\ -0.82;\ -0.51;\ 0.25\}$.

The polarization ellipse is turned as in the previous case, and $b/a = 0.12$

$\mathbf{s}_4 = 0.97\{1;\ -0.37;\ -0.67;\ 0.52\}$, $P = 0.92$,

$\mathbf{s}_{4,p} = \{1;\ -0.40;\ -0.72;\ 0.56\}$.

In this case the polarization ellipse is less elongated, $b/a = 0.3$. The big diameter is turned to the same side as in the previous cases, but by a larger angle 30°. The big polarization degree of the scattered radiation completely contradicts the above examples, in which the circularly polarized radiation was depolarized to a larger degree. One can assume that the polarization degree for scattering of such radiation increases as the ordering parameter k increases. In any case, it is observed in all the three examples of BSPM considered.

Theoretical estimates performed in the frameworks of the model assuming the polar of the column axes to be concentrated, on the average, near $\theta = \pi/2$, show significant variations of the second Stokes parameter q at the angle of preferred orientation of 45° for the particles with the diameter comparable with the radiation wavelength. Then the resonance peaks are observed, in which q varies from the values close to +1 in the case of very small particles, to –0.5 for the particles with the diameter of 3λ (Ref. 9).

If the value $q = -0.6$ obtained in the experiment is interpreted from this standpoint, one should assume very narrow size-distribution of particles, that seems to be hardly probable. In addition, the azimuth angle of the preferred orientation is significantly less than 45°. It made us to suppose that, possibly, the transformation of the parameter q observed is connected with the preferred orientation at the polar angle θ different from $\pi/2$.

Under certain conditions one can simulate this situation by tilting the lidar optical axis. Figure 5 shows the results of one of the experiments, in which only the second Stokes parameters q was measured at two mutually orthogonal linear polarizations of the laser radiation $\mathbf{s}_{01} = \{1\ 1\ 0\ 0\}^{\mathrm{T}}$ and $\mathbf{s}_{02} = \{1{-}100\}^{\mathrm{T}}$ and different angles of the lidar optical axis orientation relative to the zenith direction.

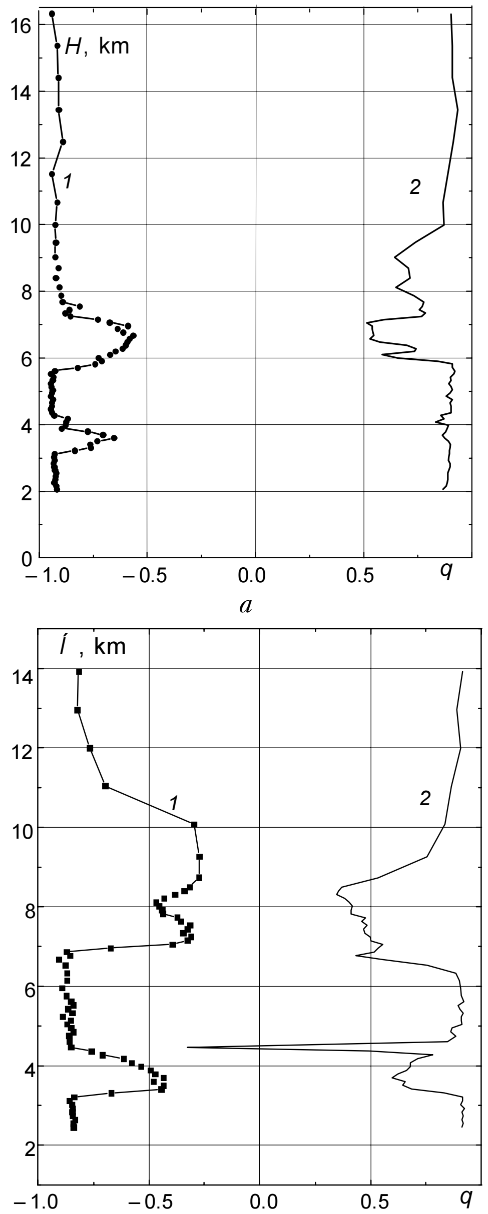

FIG. 5. Profiles of the second Stokes parameter q, measured at two polarization states of the laser beam $\mathbf{s}_{01} = \{1\ 1\ 0\ 0\}$ *(curve 2) and* $\mathbf{s}_{02} = \{1{-}100\}$ *(curve 1), a) sounding in zenith direction, b) sounding at the zenith angle of* 30°.

Profiles of the normalized parameters q obtained at sounding at zenith are shown in Fig. 5. Let us pay attention to the layer at the altitude of 3.5 km. The values of the parameter q for this layer are essentially different at different polarizations of the laser radiation, that is evidence of a significantly large value of the BSPM element $m_{12} = 0.4$ and, hence, of the presence of preferred orientation with respect to the azimuth angle. Comparing Figs. 5*a* and *b*, one can see, how the profiles of parameter q are transformed at the change of the lidar axis orientation. There occurs general decrease of the absolute values of the parameter q, that one could expect based on the general ideas, since additional asymmetry on the polar angle is introduced into the scattering ensemble.

The sharp peak in the upper part of the layer under consideration, where the parameter q crosses the zero angle into the range of the negative values, is of particular interest. We think that, this fact confirms the aforementioned assumption on the influence of the preferred orientation over the polar angle on the results of sounding shown in Fig. 4. Our next steps in this way we connect with simulating the scattering on the ensembles, which have the asymmetry in the distribution of particle axes over the polar angle.

As follows from the above, orientation of the particles in crystal clouds is a usual phenomenon, and it essentially affects the light scattering, so that the concepts of the backscattering coefficient and the lidar depolarization become ambiguous and depend on the lidar position relative to the cloud. Correct investigation of the crystal clouds by means of lidars should take into account this circumstance.

ACKNOWLEDGMENT

The work has been done using the "Lidar" setup under the financial support from Ministry of Science and Technical Policy of Russian Federation.

REFERENCES

1. O.A. Volkovitskii, L.N. Pavlova, and A.G. Petrushin, *Optical Properties of Crystal Clouds* (Gidrometeoizdat, Leningrad, 1984), 188 pp.
2. B.V. Kaul', O.A. Krasnov, A.L. Kuznetsov, and I.V. Samokhvalov, Atmos. Oceanic Opt. **4**, No. 4, 303–306 (1991).
3. B.V. Kaul', A.L. Kuznetsov, E.R. Polovtseva, and I.V. Samokhvalov, Atmos. Oceanic Opt. **6**, No. 4, 257–261 (1993).
4. B.V. Kaul', A.L. Kuznetsov, and I.V. Samokhvalov, Atmos. Oceanic Opt. **7**, No. 1, 4–7 (1994).
5. D.I. Shelefontyuk, Atmos. Oceanic Opt. **8**, No. 9, 737–739 (1995).
6. R.F. Rakhimov and D.N. Romashov, Atmos. Oceanic Opt. **4**, No. 10, 707–710 (1991).
7. D.N. Romashov and R.F. Rakhimov, Atmos. Oceanic Opt. **6**, No. 8, 515–518 (1993).
8. H.C. Van de Hulst, *Light Scattering by Small Particles* (Willey, New York, 1957).
9. R.F. Rakhimov and D.N. Romashov, Atmos. Oceanic Opt. **5**, No. 5, 287–291 (1992).